JOURNAL OF CATALYSIS 120, 377–386 (1989)

Catalytic Properties of $BaMAl_{11}O_{19-\alpha}$ (M = Cr, Mn, Fe, Co, and Ni) for High-Temperature Catalytic Combustion

MASATO MACHIDA, KOICHI EGUCHI, AND HIROMICHI ARAI

Department of Materials Science and Technology, Graduate School of Engineering Sciences, Kyushu University 39, 6-1, Kasuga-koen, Kasuga, Fukuoka 816, Japan

Received May 2, 1989; revised July 3, 1989

Series of cation-substituted barium hexaaluminates, $BaMAl_{11}O_{19-\alpha}$, (M = Cr, Mn, Fe, Co, and Ni), were investigated as catalysts for high-temperature combustion. Cation-substituted barium hexaaluminates showed high sintering resistance and retained a large surface area above 10 m^2/g even after heating at 1300°C. Transmission electron microscopic observation revealed that anisotropic crystal growth is the reason for the high heat resistance of the hexaaluminate. Manganese-substituted barium hexaaluminate, $BaMnAl_{11}O_{19-\alpha}$, was most active for CH_4 combustion. From temperature-programmed desorption of oxygen and thermogravimetric analysis of oxidation states of substituted cations, it was concluded that the catalytic activity was accelerated by oxygen sorption accompanied by reduction–oxidation of M in the hexaaluminate lattice. Accordingly, the catalytic activity of $BaMAl_{11}O_{19-\alpha}$ is approximately regulated by the difference between the heats of formation of sesquioxides of M from monoxide, i.e., $(\Delta H_f^\circ(MO_{1.5}) - \Delta H_f^\circ(MO))$, which is minimum at M = Mn. The catalytic activity of the $BaMn_xAl_{12-x}O_{19-\alpha}$ system was measured as a function of Mn content. However, the large area and high catalytic activity were obtained only when the amount of Mn was small enough to not destroy the single phase of hexaaluminate. Retention of large surface area is the most prominent feature for high-temperature catalytic combustion.

INTRODUCTION

In the past several years, much interest has arisen in the new application of catalytic combustion to gas turbines operated above 1300°C (*1–3*). The use of catalysts facilitates controllable combustion of various fuels, less emission of pollutants, and high efficiency of energy recovery. Despite many advantages, the main problem is still how to fabricate a heat-resistant catalyst. Noble metal catalysts, such as Pd and Pt, which are mainly used for combustion below 1000°C, should be excluded because of high volatility above 1300°C (*4*). Thus, there has been much interest in metal oxide catalysts because some of them have sufficient heat resistance for high-temperature applications. Some perovskite-type oxides are known to be very active oxidation catalysts (*5–7*). However, sintering at high temperatures accompanies the serious decrease in surface area (*8*). Dispersion of active metal oxides on support materials is necessary to obtain a large reaction surface at high temperatures. Barium hexaaluminate, $BaAl_{12}O_{19}$, derived from mixed metal alkoxides, is known to retain the large surface area above 1400°C that is suitable for a heat resistant support (*9, 10*). The surface area of $BaAl_{12}O_{19}$ (ca. 10 m^2/g) is 10 times larger than that of Al_2O_3 after calcination at 1600°C. The crystal structure of $BaAl_{12}O_{19}$ is a "layered aluminate type" which is known as β-alumina and magnetoplumbite types (*11, 12*). Since other hexaaluminates, such as $SrAl_{12}O_{19}$, $CaAl_{12}O_{19}$, and $LaAl_{11}O_{17}$, also show the same property (*9, 13*), the high heat resistance seems to originate from the crystal structure.

We have previously discussed a method of introducing active components for combustion into the hexaaluminate matrix (*14*). The surface area significantly decreased at

0021-9517/89 $3.00

high temperatures with the solid-state reaction in perovskite oxide supported on $BaAl_{12}O_{19}$. On the other hand, cation-substituted barium hexaaluminates, $BaMAl_{11}O_{19-\alpha}$ (M = Cr, Mn, Fe, Co, and Ni), generally retain surface areas as large as that of $BaAl_{12}O_{19}$. Since the hexaaluminate structure is thermally stable, deactivation was prevented even at high temperatures.

This study reports on the heat resistance and catalytic activity of the cation-substituted $BaAl_{12}O_{19}$. Particularly, the Mn-substituted system was investigated as the best catalyst of this series. The heat resistance and catalytic activity were characterized by microscopic observation and oxygen sorption properties, respectively.

EXPERIMENTAL

Catalyst preparation. Series of cation-substituted as well as unsubstituted barium hexaaluminates, $BaMAl_{11}O_{19-\alpha}$ (M = Al, Cr, Mn, Fe, Co, and Ni) were prepared by the hydrolysis of metal alkoxides. Barium isopropoxide ($Ba(OC_3H_7)_2$) was obtained by reaction between Ba metal (99%, Kishida Chemical) and 2-propanol in a nitrogen stream. Calculated amounts of $Ba(OC_3H_7)_2$ and $Al(OC_3H_7)_3$ (99%, Kishida Chemical) were dissolved in 2-propanol and were kept in 80°C for 5 h. An aqueous solution of acetate or nitrate of transition metals was added to the alcoholic solution of metal alkoxides. The precipitate thus formed with gelation was evaporated to dryness. All samples were calcined at 1300°C prior to their use for catalytic reaction. The crystal structures of calcined samples were determined by X-ray diffraction (Rigaku Denki, 4011) with Cu$K\alpha$ radiation. The specific surface areas of calcined samples were measured by the BET method using N_2 adsorption.

Transmission electron microscopy (TEM). A transmission electron microscope (JOEL, JEM-2000FX) was used for imaging, energy dispersive X-ray spectroscopy (EDS, Tracor Northern TN-2000), and selected area diffraction in TEM mode operating at 200 kV.

Catalytic combustion of methane. Catalytic activities were measured in a conventional flow system under atmospheric pressure. Catalysts were fixed in a quartz reactor by packing alumina beads at both ends of the catalyst bed. A gaseous mixture of methane (1 vol%) and air (99 vol%) was fed to the catalyst bed at a flow rate of 48000 $cm^3\ h^{-1}$ (space velocity = 48000 h^{-1}). The methane conversion in the effluent gas was analyzed by on-line gas chromatography. The combustion activity is expressed as temperatures, $T_{10\%}$ and $T_{90\%}$, at which conversion levels of 10 and 90%, respectively, are attained.

Temperature-programmed desorption (TPD) of oxygen. Temperature-programmed desorption (TPD) of oxygen was measured in a flow system. Prior to the measurement, the sample was treated in a oxygen stream (50 ml/min) at 800°C for 1 h and subsequently cooled to room temperature. After evacuation, helium was introduced into the system and the sample was heated at a constant rate of 10°/min in a He stream (50 ml/min). Desorbed oxygen in effluent gas was detected by a TCD cell.

Thermogravimetry (TG). The oxidation states of transition elements (Mn, Fe, Co, and Ni) in the hexaaluminate structure were determined by thermogravimetry (Shimadzu DT-40) equipped to a flow system. Prior to measurement, a sample was heated at 1000°C in dry air to remove physisorbed water and then cooled to room temperature. After evacuation, the sample was heated again at a constant rate of 10°/min in a H_2 stream (30 ml/min) up to 1100°C. The weight loss of the sample corresponds to the degree of reduction.

RESULTS

Surface, Area, Crystal Structure, and Microstructures

After calcination at 1300°C, cation-substituted samples ($BaMAl_{11}O_{19-\alpha}$) were com-

posed of hexaaluminate phase, but the unsubstituted single oxides were hardly detected by X-ray diffraction. Since transition metal ions occupy Al sites in the hexaaluminate structure, the diffraction lines shifted to angles lower than those of $BaAl_{12}O_{19}$. The surface areas of Ba $MAl_{11}O_{19-\alpha}$, which were lowered by the substitution, were still large, ranging between 10 and 15 m^2/g (Table 1).

Figure 1a shows TEM photographs of $BaMnAl_{11}O_{19-\alpha}$ after calcination at 1300°C. The sample consisted of highly dispersed planar crystallites 100–200 nm in diameter and ca. 20 nm thick. The crystal orientation was determined by selected area diffraction (SAD) as shown by "×" in Fig. 1a. The planar facets have orientations parallel to the (001) plane of the hexaaluminate structure. The crystal habit is the same as unsubstituted $BaAl_{12}O_{19}$, in which the crystal growth is strongly suppressed along the *c* axis as reported previously (*15*). Mn-substitution in the hexaaluminate lattice was evidenced by the EDS spectrum taken from one of the crystals (Fig. 1b). The chemical composition calculated from integration of the spectrum agreed with that of the starting material.

TABLE 1

Surface Areas and Methane Combustion Activities of $BaMAl_{11}O_{19-\alpha}$

M	Surface area[a] m^2/g	$T_{10\%}$[b] (°C)	$T_{90\%}$[b] (°C)
Al	15.3	710	730
Cr	15.7	700	770
Mn	13.7	540	740
Fe	11.1	560	780
Co	15.2	690	720
Ni	11.1	710	770
Thermal reaction[c]		810	860

[a] After calcination at 1300°C.

[b] Temperatures at which conversion levels are 10 and 90%.

[c] An empty reactor packed with alumina beads.

Catalytic Activities for Methane Combustion

Combustion activities of the cation-substituted samples are summarized as $T_{10\%}$ and $T_{90\%}$ in Table 1. When an empty reactor packed with alumina beads was submitted to the reaction, combustion appears to be initiated by the radical formation at the surface of alumina beads and to progress through chain reaction in the gas phase, as can be characterized by the high initiation temperature ($T_{10\%}$) and the steep rise in CH_4 conversion. The combustion behavior over unsubstituted and Co-, Ni-, or Cr-substituted samples is similar to that of the empty reactor, since the catalytic activities of these transition metal ions appear to be very small in the hexaaluminate lattice. However, the initiation temperatures were significantly lowered by employing the catalyst with large surface area which is effective in promoting the radical reaction. The Fe- and Mn-substituted samples catalytically initiate the reaction at lower temperature ($T_{10\%}$ = 540–560°C). The lowest $T_{10\%}$ values (540°C) was attained by BaMn $Al_{11}O_{19-\alpha}$, which also showed relatively high activity at a high conversion level ($T_{90\%}$). Table 1 indicates that the low $T_{90\%}$ value is not always obtained for the samples with high catalytic activity. This is because the overall reaction over active catalysts (M = Mn, Fe) was limited by the mass transfer at the high conversion level. The reaction products were carbon dioxide and water except for carbon monoxide, which was dominant when the radical reaction took place.

The catalytic activity of Mn-substituted hexaaluminate is compared to that of perovskite-type oxide, $LaCoO_3$, which is known as one of the active combustion catalysts. Table 2 shows the rates of methane oxidation at 500°C which are expressed per unit surface area and per catalyst mass. The activity per unit surface area is notably low for $BaMnAl_{11}O_{19-\alpha}$, whereas the activities of the two catalysts are comparable per unit

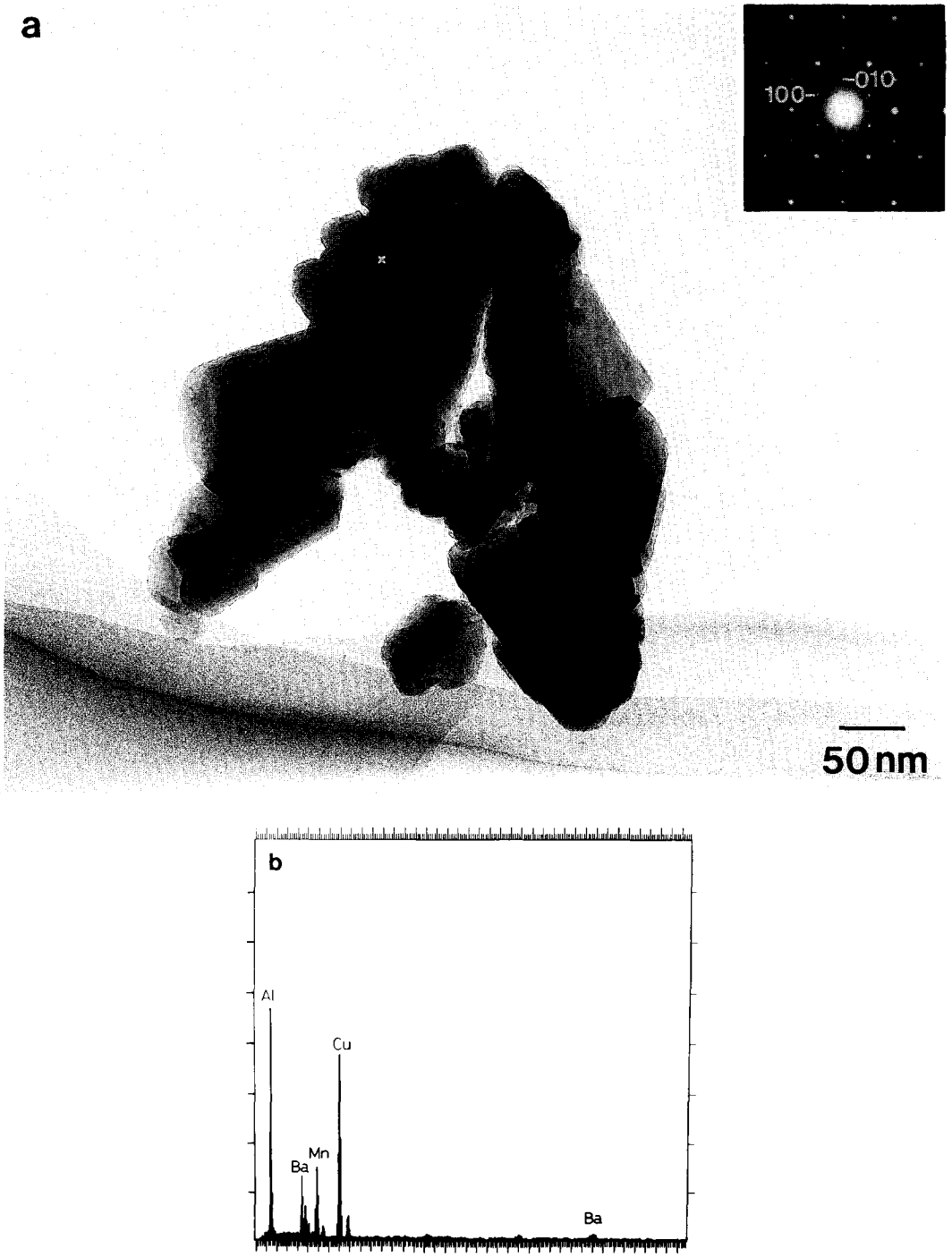

FIG. 1. TEM micrograph (a) and EDS spectrum (b) of $BaMnAl_{11}O_{19-\alpha}$ after calcination at 1300°C. A Cu peak is from microscope grids.

TABLE 2

Relative Catalytic Activity of $BaMnAl_{11}O_{19-\alpha}$ and $LaCoO_3$ at 500°C

	Reaction rate	
	Per unit surface area (mol m^{-2} h^{-1})	Per unit mass (mol g^{-1} h^{-1})
$BaMnAl_{11}O_{19-\alpha}$	0.012	0.169
$LaCoO_3$	0.351	0.105

mass. This means that the high catalytic activity of $BaMnAl_{11}O_{19-\alpha}$ results from the large surface area. As was observed by TEM, the planar crystallites with large aspect ratio correspond to the large reaction surface per unit mass, which appears to be quite effective for catalytic combustion.

Temperature-Programmed Desorption (TPD) of Oxygen

Figure 2 shows TPD profiles of oxygen from $BaMAl_{11}O_{19-\alpha}$. The rate of oxygen desorption was plotted as a function of catalyst temperature. Oxygen desorption was observed for cation-substituted samples but not for $BaAl_{12}O_{19}$ up to 1000°C. The catalysts can be classified into two groups from their desorption patterns. Oxygen desorption from the first group, with M = Cr, Co, and Ni, was extremely small. The catalysts in this group showed low catalytic activity for methane combustion (Table 1). The second group, i.e., Mn- and Fe-substituted systems, is active for CH_4 combustion. A large amount of oxygen was desorbed at high temperatures (>500°C). The desorption from $BaFeAl_{11}O_{19-\alpha}$ started at about 600°C and the peak of the desorption rate was located above 900°C. The desorption from the $BaMnAl_{11}O_{19-\alpha}$ sample was rather small and was located at a low temperature (850°C). These results indicate that the catalytic activity of hexaaluminate catalysts is related to the large amount of oxygen, which is bonded to the substituted cations in the hexaaluminate lattice.

Oxidation State of M in $BaMAl_{11}O_{19-\alpha}$

In order to determine the oxidation states of M, the weight loss accompanied by reduction of $BaMAl_{11}O_{19-\alpha}$ was measured by *in situ* thermogravimetry (TG). With heating up to 1100°C in a H_2 flow, Fe, Co, and Ni ions are reduced into their metallic states, and only Mn is reduced into the divalent state. Thus, reduction of cation-substituted hexaaluminate is expressed as

$$BaMAl_{11}O_{19-\alpha} + (1.5 - n - \alpha)H_2 \rightarrow MO_n + BaAl_{11}O_{17.5} + (1.5 - n - \alpha)H_2O,$$

where $n = 0$ for M = Fe, Co, and Ni and $n = 1.0$ for Mn. The initial oxidation state of M is calculated from the weight loss and the final oxidation states after reduction from the equation

$$\text{oxidation state} = 2n + 2\Delta W(714.12 + M_w + 16n)/[16W(1 - \Delta W/W)],$$

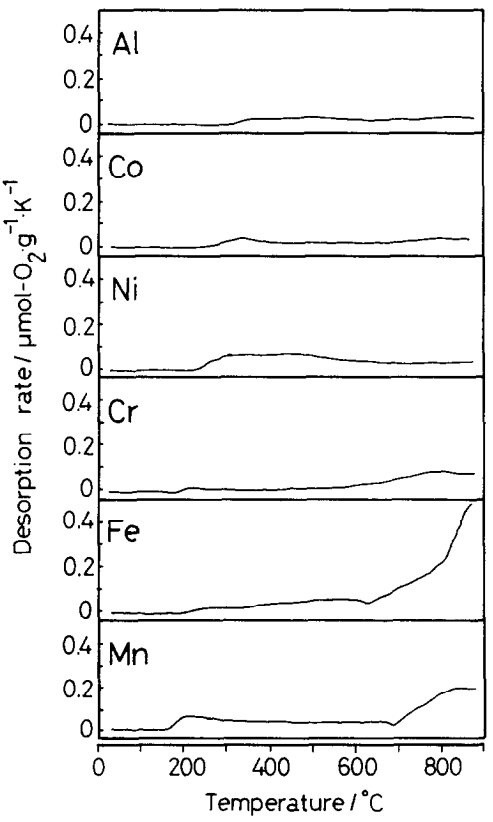

FIG. 2. TPD profiles of oxygen from $BaMAl_{11}O_{19-\alpha}$.

TABLE 3

Average Oxidation State of M in $BaMAl_{11}O_{19-\alpha}$

M	Average oxidation state
Cr	3.0
Mn	2.4
Fe	3.0
Co	2.1
Ni	2.0

where ΔW is the weight loss, W, the initial sample weight, and M_w, atomic weight of M. The average valence states of M thus calculated are listed in Table 3. Although $BaCrAl_{11}O_{19-\alpha}$ is too stable to be reduced by H_2 up to 1100°C, the oxidation state of Cr is thought to be +3.0 as reported for $LaMgAl_{11-x}Cr_xO_{19}$ by Vivien *et al.* (*16*). Cobalt and nickel are both in the divalent state, but Fe is in the trivalent state. The average oxidation number of Mn (+2.4) indicates the mixed valence state of Mn^{2+} and Mn^{3+} in the hexaaluminate lattice.

Surface Area and Combustion Activity of $BaMn_xAl_{12-x}O_{19-\alpha}$

The crystal structure of the Mn-substituted system was investigated by X-ray diffraction as a function of atomic fraction of Mn in $BaMn_xAl_{12-x}O_{19-\alpha}$. The lattice constant of the hexaaluminate structure increased with substitution of Mn ions for Al^{3+} sites at $x < 3.0$ (Fig. 3). Further addition of Mn at $x > 3.0$ did not change the lattice constant, but a second phase, $BaAl_2O_4$, appeared. The result indicates that the samples at $x < 3.0$ are homogeneous solid solutions of hexaaluminate but those at $x > 3.0$ are mixtures of hexaaluminate phase and $BaAl_2O_4$.

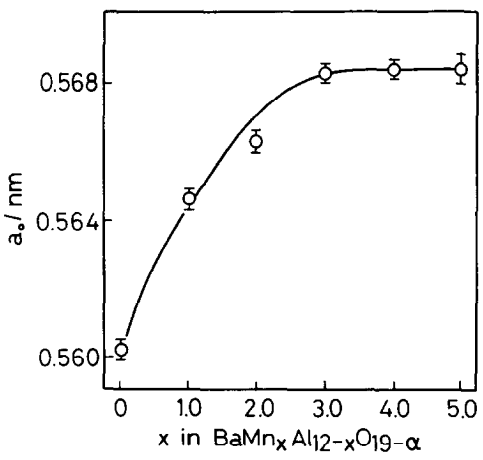

FIG. 3. The lattice constant of $BaMn_xAl_{12-x}O_{19-\alpha}$ after calcination at 1300°C.

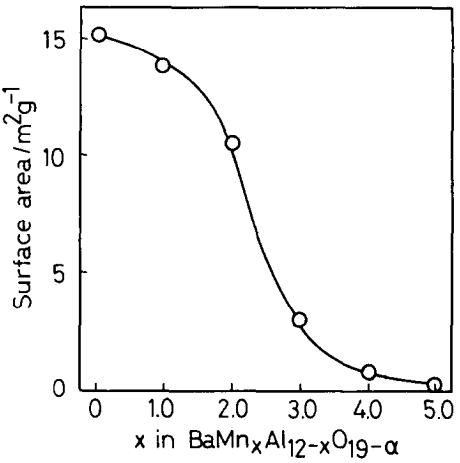

FIG. 4. The surface area of the $BaMn_xAl_{12-x}O_{19-\alpha}$ system after calcination at 1300°C.

Figure 4 shows the change in surface areas of $BaMn_xAl_{12-x}O_{19-\alpha}$ calcined at 1300°C. Although the surface area decreased unvaryingly with x, the decrease was gradual at $x < 2.0$. At this composition, the sample consisted of the hexaaluminate phase. In contrast, the surface area was steeply reduced as the second phase of $BaAl_2O_4$ precipitated at $x > 2.0$.

The catalytic activity for methane combustion over $BaMn_xAl_{12-x}O_{19-\alpha}$ is tested as a function of x in Fig. 5. The initiation temperature of combustion was reduced with the partial substitution of Mn up to $x = 2.0$. However, the catalyst became less active, especially at the high conversion level, with a further substitution at $2.0 < x < 4.0$ because of the significant decrease in surface area.

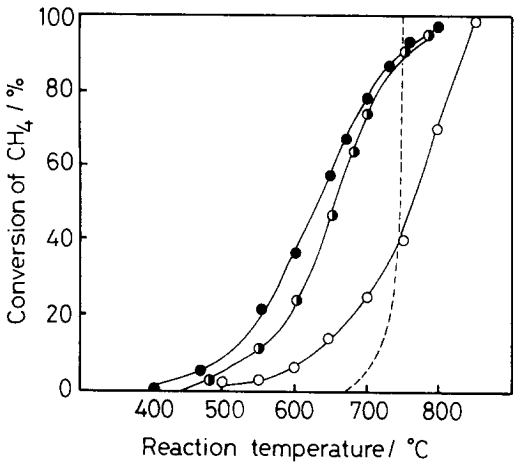

FIG. 5. Catalytic combustion of methane over $BaMn_xAl_{12-x}O_{19-\alpha}$:

	x	Surface area/$m^2 \cdot g^{-1}$
----	0	15.3
◑	1.0	13.7
●	2.0	10.4
○	4.0	0.9

DISCUSSION

Relation between Large Surface Area and Crystal Structure

The crystal structure of hexaaluminate belongs to β-alumina or magnetoplumbite type. Barium hexaaluminate is classified as β-alumina type in Fig. 6 (*17, 18*). This structure consists of oxygen in close-packed spinel blocks separated by mirror planes along the *c* axis. The mirror planes contain large cations such as Ba^{2+} and loosely packed oxygen. The layered crystal structure of hexaaluminate is retained for Ba $MAl_{11}O_{19-\alpha}$ in which one Al site per double spinel block is occupied by an M ion.

TEM observation revealed that Mn-substituted hexaaluminate was obtained as planar crystallite in which the flat surface oriented parallel to the (001) plane. This anisotropic shape of the crystallites suggests that crystal growth along the *c* axis is strongly suppressed compared to that along the direction normal to the *c* axis; i.e., crystal growth by stacking of each spinel block along the *c* axis is very slow. Such crystal morphology is also reported for barium hexaaluminate (*15*) and is a common feature of hexaaluminate-related compounds.

Catalytic Properties for High-Temperature Catalytic Combustion

High catalytic activity is an indispensible factor for ignition to occur at the lowest possible temperature. At high temperatures, however, the surface reaction proceeds so immediately that the overall reaction is limited by the mass transfer of reactants to the catalyst surface from the gas phase. Maintaining the large surface area of combustion catalysts is important in

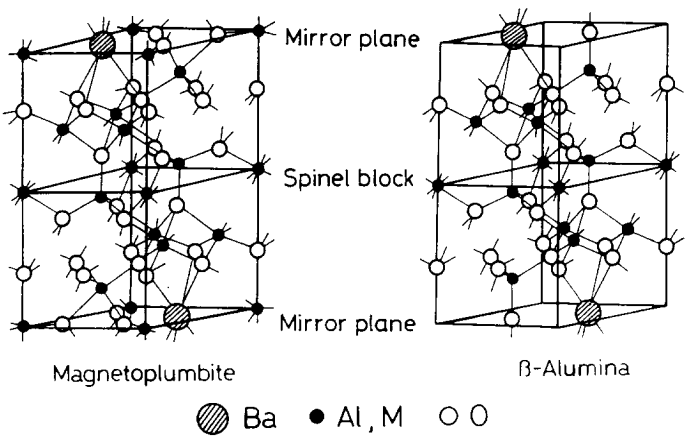

FIG. 6. Crystal structures of hexaaluminates.

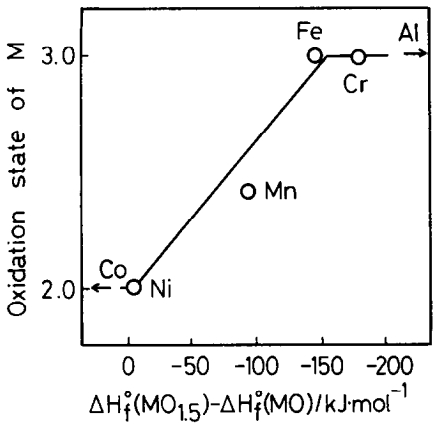

FIG. 7. Relation between the oxidation state of M in $BaMAl_{11}O_{19-\alpha}$ and $(\Delta H_f^\circ(MO_{1.5}) - \Delta H_f^\circ(MO))$.

promoting the reaction under the mass transfer limitation. Large surface area is also effective in initiating the reaction over less active catalysts (M = Al, Cr, Co, and Ni) as can be seen from a comparison with the reaction in an empty reactor (Table 1). In these systems, the combustion proceeds via homogeneous gas-phase reaction initiated by radical formation at the catalyst surface. The large surface area appears to significantly promote the radical formation.

These results conclude that the large surface area plays an important role in catalytic and homogeneous combustion. Both the catalytic activity and the large surface area are indispensable to the high-temperature catalytic combustion, but no materials reported so far satisfy these requirements when used at high temperatures. The Mn-substituted hexaaluminate is the first material which attains simultaneously the catalytic activity and the heat resistance necessary to maintain a large surface area.

Relation between Catalytic Activity and Oxidation State of M

Determination of the oxidation states of transition elements, M, from *in situ* TG measurements was the first quantitative analysis of the present system, although those in the $LaMAl_{11}O_{19}$ single crystal have already been studied (*19, 20*). Table 3 shows that all the transition elements were in di- or trivalent states. The sequence of the oxidation states appears to be related to the bonding strength between metal and oxygen, which is roughly estimated as the standard heat of formation of oxides, $\Delta H_f^\circ(MO_n)$. The heat of MO_x formation decreases with increasing the number of $3d$ electrons. In the metal cations of interest, only divalent, trivalent, or mixed valence states are considered to be possible. Figure 7 shows the relation between the average oxidation state of M and $(\Delta H_f^\circ(MO_{1.5}) - \Delta H_f^\circ(MO))$. In this case, $\Delta H_f^\circ(CoO_{1.5})$ is calculated from the Born–Haber cycle by assuming that the lattice energy of Co_2O_3 is equal to that of Fe_2O_3. It is apparent that Co and Ni with low $(\Delta H_f^\circ(MO_{1.5}) - \Delta H_f^\circ(MO))$ prefer the divalent state, but Fe and Cr with high $(\Delta H_f^\circ(MO_{1.5}) - \Delta H_f^\circ(MO))$ prefer the trivalent state in the hexaaluminate. Manganese ions are in the intermediate state between 2.0 and 3.0 as shown in Table 2. The trivalent Mn ions were also observed in single-crystal La-hexaaluminate by ESR and absorption spectra when the sample was reduced with H_2 and subsequently annealed in air (*19*). This result is consistent with the quantitative analysis of the present study.

The catalytic activities of $BaMAl_{11}O_{19-\alpha}$ were reflected by their TPD profiles (Fig. 2). Oxygen species, which were desorbed from the Mn- and Fe-substituted samples above 500°C, appear to be active for methane combustion. The oxygen desorption accompanies the reduction of transition elements, M, in the hexaaluminate lattice because no desorption peaks appeared without metal substitution. The oxygen desorption from $BaMAl_{11}O_{19-\alpha}$ (M = Mn, Fe) corresponds to the partial reduction of M^{3+} to M^{2+}. Since reduced Mn or Fe species (divalent state) are reoxidized easily in O_2 flow, an exothermic peak was observed when the catalyst was heated in air after TPD measurement. As for systems of M = Cr, Co, and Ni, amounts of oxygen desorption were as small as that from unsubstituted barium hexaaluminate. This result indicates that the oxidation states of these ions (Cr^{3+}, Co^{2+}, and Ni^{2+}) are too stable in

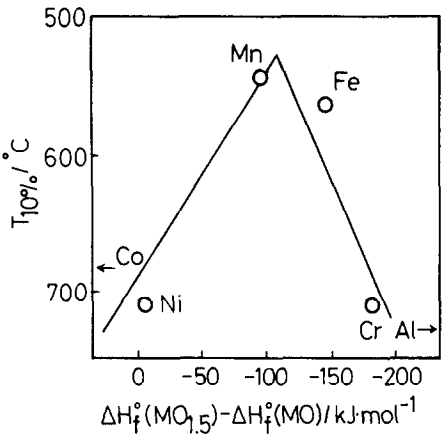

FIG. 8. Relation between the catalytic activity of $BaMAl_{11}O_{19-\alpha}$ and $(\Delta H_f^\circ(MO_{1.5}) - \Delta H_f^\circ(MO))$.

the hexaaluminate lattice to contribute to the redox cycle.

A sequence of catalytic activity ($T_{10\%}$) of $BaMAl_{11}O_{19}$ (Table 1) is apparently different from that of the single oxide of M. A correlation between catalytic oxidation activity of single metal oxides and the heats of formation of the oxides has been proposed by several researchers (*21–24*). Here, we assume that the catalytic oxidation of methane proceeds via the following reduction/oxidation cycle of M between di- and trivalent in the hexaaluminate lattice:

$$MO + \tfrac{1}{4}O_2 \rightarrow MO_{1.5}$$

$$MO_{1.5} + \tfrac{1}{8}CH_4 \rightarrow MO + \tfrac{1}{8}CO_2 + \tfrac{1}{4}H_2O$$

The reversibility of the reduction/oxidation cycle between MO and $MO_{1.5}$ can be estimated by $(\Delta H_f^\circ(MO_{1.5}) - \Delta H_f^\circ(MO))$. The catalytic activity ($T_{10\%}$) of $BaMAl_{11}O_{19-\alpha}$ is plotted against this parameter in Fig. 8. It is apparent that the activity is well summarized by a volcano-like relation with $(\Delta H_f^\circ(MO_{1.5}) - \Delta H_f^\circ(MO))$. The relation indicates that the reduction of $MO_{1.5}$ into MO is the slowest step in methane oxidation over the catalysts located on the right arm. Thus, catalytic activity decreases with the increasing stability of $MO_{1.5}$ states. In contrast, the oxidation of MO into $MO_{1.5}$ is rather difficult and the catalytic activity decreases with the increasing stability of MO states in the left arm of Fig. 8. Based on this volcano-like relation, manganese ions play a key role in the reduction/oxidation cycle with the lowest energy, and this will probably be very effective in methane oxidation.

Structural Modification of the Mn-Substituted System

In order to enhance catalytic performance, we have examined the dependence of Mn-content on surface area and on catalytic activity. A variety of transition elements are easily incorporated into hexaaluminate as has been reported by Laville and Lejus (*25*), but the solubility limits have not been studied so far. The Al sites in barium hexaaluminate cannot be replaced completely by Mn (Fig. 3). The $BaMn_xAl_{12-x}O_{19-\alpha}$ sample consists of single hexaaluminate at $x < 3.0$ and of a mixture of hexaaluminate and a $BaAl_2O_4$-like phase at $x > 3.0$ after calcination at 1300°C. The surface area of $BaMn_xAl_{12-x}O_{19-\alpha}$ strongly depends on the crystalline phase. With increasing Mn content, the surface area decreased gradually at $x < 2.0$, but the precipitation of the second phase significantly lowered the surface area. The crystallite sizes of the two phases obtained by X-ray line broadening analysis of $BaMn_xAl_{12-x}O_{19-\alpha}$ were 10–50 nm for the hexaaluminate and 100 nm for the $BaAl_2O_4$-like phase (Fig. 9). Although the hexaaluminate structure is effective in retaining a large surface area, $BaAl_2O_4$ does not contribute to this effect (*9*). Thus, cation substitution in barium hexaaluminate does not lead to any serious reduction of surface area when the single phase of hexaaluminate is retained.

The combustion activity of the $BaMn_xAl_{12-x}O_{19-\alpha}$ system also depends on the composition as shown in Fig. 5. At $x < 3.0$, the catalytic activity increased with Mn content because of the increase in population of the active sites, which contribute to the reduction/oxidation reaction. However, the catalytic activity is appreciably lowered by the decrease in surface area at $x > 3.0$ where the second phase with large crystal-

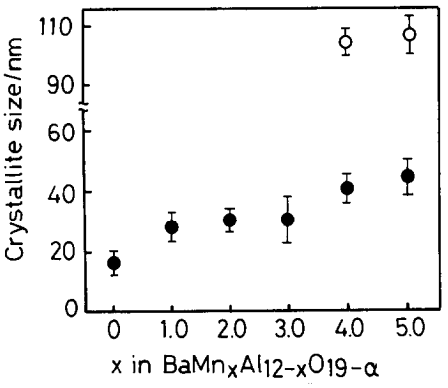

FIG. 9. Average crystallite sizes of $BaMn_xAl_{12-x}O_{19-\alpha}$ obtained from the line broadening analysis of X-ray diffraction. (●) $BaAl_{12}O_{19}$-like phase; (○) $BaAl_2O_4$-like phase.

lite size appeared. Since the relative activity per unit surface area is rather low in Mn-substituted hexaaluminate, as was revealed in Table 2, Mn content, x, should be low enough to retain a large surface area.

CONCLUSION

The present study revealed that the cation-substituted hexaaluminates possess the potential heat resistance of a high-temperature combustion catalyst. The large surface area after calcination at 1300°C is caused by the suppression of crystal growth along the c axis as was shown by electron microscopy. The Mn-substituted hexaaluminate provides the best catalytic activity for methane combustion only when the single phase of hexaaluminate is retained. The catalytic activity of cation-substituted hexaaluminates seems to be related to the reduction/oxidation behavior of transition elements in the crystal lattice. The reduction/oxidation cycle of manganese, which is reversible between di- and trivalent states in the hexaaluminate lattice, leads to high catalytic activity for methane combustion.

ACKNOWLEDGMENT

The electron microscopic experiments in this study were carried out in the High Voltage Electron Microscopy Laboratory of Kyushu University.

REFERENCES

1. Trimm, D. L., *Appl. Catal.* **7,** 249 (1983).
2. Prasad, R., Kennedy, L. A., and Ruckenstein, E., *Catal. Rev.* **26,** 1 (1984).
3. Pfefferle, L. D., and Pfefferle, W. C., *Catal. Rev.* **29,** 219 (1987).
4. Alcock, C. B., and Hooper, G. W., *Proc. Soc. A* **254,** 551 (1960).
5. Libby, W. F., *Science* **171,** 499 (1971).
6. Voorhoeve, R. J. H., and Remeika, J. P., *Ann. N.Y. Acad. Sci.* **272,** 3 (1976).
7. Nakamura, T., Misono, M., Uchijima, T., and Yoneda, Y., *Nippon Kagaku Kaishi* **1980,** 1679 (1980).
8. Arai, H., Yamada, T., Eguchi, K., and Seiyama, T., *Appl. Catal.* **26,** 265 (1986).
9. Machida, M., Eguchi, K., and Arai, H., *J. Catal.* **103,** 385 (1987).
10. Machida, M., Eguchi, K., and Arai, H., *Bull. Chem. Soc. Japan* **61,** 3659 (1988).
11. Verstegen, J. M. P. J., and Steevels, A. L. N., *J. Lumin.* **9,** 406 (1974).
12. Steevels, A. L. N., and Schrama-de Pauw, A. D. M., *J. Electrochem. Soc.* **125,** 691 (1976).
13. Matsuda, S., Kato, S., Mizumoto, M., and Yamashita, H., *in* "Proceedings, 8th International Congress on Catalysis, Berlin, 1984," Vol. 4, p. 879. Dechema, Frankfurt-am-Main, 1984.
14. Machida, M., Eguchi, K., and Arai, H., *Chem. Lett.* **1987,** 767 (1987).
15. Machida, M., Eguchi, K., and Arai, H., *J. Am. Ceram. Soc.* **71,** 1142 (1988).
16. Viana, B., Lejus, A. M., Vivien, D., Poncon, V., and Boulon, G., *J. Solid State Chem.* **71,** 77 (1987).
17. Kimura, S., Bannai, E., and Shindo, I., *Mater. Res. Bull.* **17,** 209 (1982).
18. Iyi, N., Inoue, Z., Takekawa, S., and Kimura, S., *J. Solid State Chem.* **52,** 66 (1984).
19. Laville, F., Gourier, D., Lejus, A. M., and Vivien, D., *J. Solid State Chem.* **49,** 180 (1983).
20. Gasperin, M., Saine, M. C., Kahn, A., Laville, F., and Lejus, A. M., *J. Solid State Chem.* **54,** 61 (1984).
21. Sabatier, P., *Ber. Dtsch. Chem. Ges.* **44,** 2001 (1911).
22. Baladin, A. A., *in* "Advances in Catalysis (D. D. Eley, H. Pines, and P. B. Weisz, Eds.), Vol. 10, p. 96. Academic Press, New York, 1958.
23. Moro-oka, Y., and Ozaki, A., *J. Catal.* **5,** 116 (1966).
24. Kagawa, S., Kajiwara, Y., Tokunaga, S., and Seiyama, T., *Shokubai* **8,** 306 (1966).
25. Laville, F., and Lejus, D., *J. Cryst. Growth* **63,** 429 (1983).